

Gram Matrices, Coherent States, and Hofstadter Butterfly with Flat Band

Youjiang Xu and Han Pu

*Department of Physics and Astronomy, and Rice Center for Quantum Materials,
Rice University, Houston, Texas 77251-1892, USA*

We propose a new principle using which Hamiltonians supporting flat band can be systematically constructed. The principle is built upon the properties of the Gram matrices. Especially, the Gram matrices of certain subsets of coherent states can be interpreted as Hamiltonians describing a charged particle hopping on a two-dimensional lattice subjected to a gauge field. The massive degeneracy of the ground states in these models is a universal property guaranteed by the (over)completeness of the coherent states, independent from the geometry of the lattice. We study the ground state wave functions and the band structure of these models. Experimental realization of the model is promising because the essential features can be seen on very small lattices.

Models that support flat bands, i.e., with single-particle energy dispersion $E(\mathbf{k})$ independent of momentum \mathbf{k} , are of great importance. The quenched kinetic energy and the associated macroscopic degeneracy in a flat band makes the system extremely sensitive to perturbations. In particular, in a many-body setting, interaction between particles in the flat band, no matter how weak it is, can result in strong correlations and exotic quantum phases. This is exactly what happens in, for example, fractional quantum Hall systems [1–3], where the underlying single-particle spectrum features flat Landau levels. It is therefore important to understand what model Hamiltonians can support flat bands and, conversely, how one can systematically generate models supporting flat bands. Previous studies have shown that flat bands can emerge as a result of different mechanisms such as topology, symmetry, or interference [4, 5]. In this work, we propose a new principle to generate flat-band models. This principle relies on the mathematical properties of the so-called Gram matrices, and the flat band it generates is guaranteed to be the lowest-energy band.

Consider a set of n vectors $|v_i\rangle$ ($i = 1, 2, \dots, n$) in a linear vector space. Together they can form a matrix \mathbf{A} whose i^{th} column is $|v_i\rangle$. The matrix $\mathbf{G} \equiv \mathbf{A}^\dagger \mathbf{A}$ is called a Gram matrix. By construction, \mathbf{G} is hermitian and positive semi-definite. The hermiticity and positivity mean that we can interpret \mathbf{G} as a Hamiltonian of certain physical system. If the set of vectors $\{|v_i\rangle\}$ are linearly independent, then \mathbf{G} is positive definite; otherwise, \mathbf{G} would possess zero eigenvalues. If the dimension of the space spanned by $\{|v_i\rangle\}$ is m , then the number of zero eigenvalues that \mathbf{G} possesses is $n - m$. If \mathbf{G} is interpreted as a Hamiltonian, then these zero eigenvalues correspond to the ground state manifold. As a result, we have a powerful principle of constructing Hamiltonians with perfectly flat ground band. We can adjust the properties of the Hamiltonian by properly choosing the vectors that the Gram matrix is built upon. In the following, we will provide a specific example where the Gram matrix is built upon a subset of coherent states. The corresponding Hamiltonian describes a charged particle hopping on a two dimensional lattice subjected to a

gauge field. The zero-energy states of this model exhibit universal properties determined by the properties of the coherent states.

A coherent state $|z\rangle$ is an eigenstate of a bosonic annihilation operator with complex eigenvalue z . The full set of coherent states form an overcomplete basis. Perelomov [6] showed that a countable subset of coherent states can form a complete basis. Such a subset can be constructed as follows. Define $z_{m,n} := m\omega_1 + n\omega_2$, $m, n \in \mathbb{Z}$, $\omega_1, \omega_2 \in \mathbb{C}$, $S := \text{Im}\omega_1^* \omega_2 > 0$. $z_{m,n}$'s form a lattice on the complex plane whose unit cell area is S . We collect the set of coherent states $\{|z_{m,n}\rangle\}$. If $S < \pi$, the set represents an overcomplete basis. If $S > \pi$, the set is incomplete. If $S = \pi$, we can take away any one of the $|z_{m,n}\rangle$'s from the set, and the remaining states form a complete basis.

The dependence of the completeness of the set on S determines the number of zero eigenvalues of the corresponding Gram matrix, denoted as G^S , built upon these coherent states. Specifically, the matrix elements of G^S are given by

$$\begin{aligned} G_{m',n';m,n}^S &:= \langle z_{m',n'} | z_{m,n} \rangle \\ &= e^{-|z_{m,n} - z_{m',n'}|^2/2 + i \text{Im} z_{m',n'}^* z_{m,n}}, \end{aligned} \quad (1)$$

The number of zero eigenvalues of G^S can be determined as follows [6]: When $S > \pi$, the set of coherent states are linear independent, and the smallest eigenvalue of the resulting G^S must be positive. When $S = \pi$, the set $\{|z_{m,n}\rangle\}$ becomes complete if we take away any one of the state, so G^S has a single zero eigenvalue. When $S < \pi$, we have $1/S$ states per unit area on the complex plane, while only $1/\pi$ states per unit area are needed to construct a complete basis, so a fraction of $1 - S/\pi$ eigenvalues of G^S are zero.

Therefore, if interpreted as a Hamiltonian, G^S produces an interesting spectrum when $S < \pi$: it features a massively degenerate zero-energy ground band. The matrix elements of G^S in Eq. (1) can be interpreted as the hopping amplitude of a particle between two lattice sites $z_{m,n}$ and $z_{m',n'}$, experiencing a constant gauge field with the flux per unit cell being $2S$. The hopping amplitude

decreases as a Gaussian function of the distance between the sites. If $\{z_{m,n}\}$ form a square lattice, G^S reduces to the model studied by Kapit and Mueller [7] up to a gauge transformation [8, 9]. If we further take $S \rightarrow \infty$, our model, after a scaling factor of $e^{S/2}$, reduces to the Hofstadter's model [10], which contains only nearest-neighbor hopping.

To give some illustration, we carry out the following numerical calculation. We choose N coherent states distributed in a square region on the complex plane, where N is large but finite (typically, $N \sim 10^3$), and numerically diagonalize the corresponding Gram matrix G^S to find the spectrum. In Fig. (1)(a)-(c), we display the spectrum for several distinct lattice geometry: square lattice, triangular lattice, and honeycomb lattice. The common feature for these different cases is the flat ground band at zero energy when $S < \pi$, with degeneracy given by $(1 - S/\pi)N$. The positive-energy part of the spectrum forms a Hofstadter butterfly, whose specific pattern depends on the lattice geometry. In Fig. (1)(d), we display the spectrum where the coherent states has a random distribution over the whole region, and we specify a lower bound on the distances between sites to ensure that never two sites are too close together in order to exclude trivial zero eigenvalues of the Gram matrix. In this case, the butterfly pattern is no longer there, but remarkably, the zero-energy flat band remains robust at $S < \pi$ (here S is defined as the average area occupied by each state). Therefore, we conclude that, when $S < \pi$, the massively degenerate zero-energy states is a universal feature of the system, to a large extent, independent of the distribution of the sites. Furthermore, the gap between the zero-energy band and the lowest excited state increases as S decreases and diverges when $S \rightarrow 0$. This can be easily understood as follows. Since $\text{Tr}[G^S] = N$ which is the sum of the positive eigenenergies, the averaged energy of the excited states should be π/S when $S < \pi$ according to the degeneracy of the ground states.

We now work out the wave functions of the zero-energy states analytically. Following a similar approach used by Kapit and Mueller for square lattice [7] and using a more general singlet sum rule [11] proved by Perelomov [6]:

$$\sum_{m,n} (-1)^{m+n+mn} e^{-\frac{|\alpha_{m,n}|^2}{2} + \alpha_{m,n}z} \equiv 0, \quad (2)$$

where z is an arbitrary complex number and $\alpha_{m,n}$'s build an arbitrary lattice whose unit cell area is π , we can prove (see Supplemental Material [9] for more details):

$$\sum_{m,n} G_{m',n';m,n}^S \phi^{(j)}(z_{m,n}) = 0, \quad (3)$$

for $S < \pi$, where:

$$\phi^{(j)}(z_{m,n}) = (-1)^{m+n+mn} z_{m,n}^j e^{-\frac{\pi/S-1}{2}|z_{m,n}|^2}. \quad (4)$$

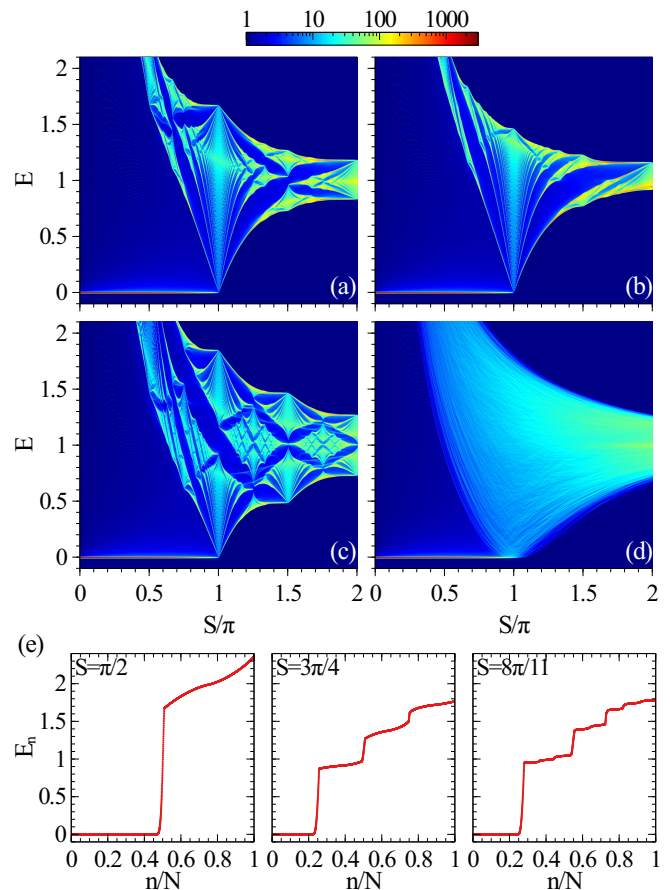


FIG. 1. (Color online) Spectrum of G^S . The color map represents $(D+1)$ where $D(E) = \sum_n \delta(E - E_n)$, with E_n being the n^{th} eigenvalue of G^S , is the density of states. In the calculation, the Dirac δ -function is replaced by a smooth narrow distribution function. We have roughly $N \approx 3600$ states distributed in a square area on the complex plane. S is the average area per state. For a regular lattice, S is just the area of the unit cell. The distribution of the coherent states for each panel: (a) Square lattice. (b) Triangular lattice. (c) Honeycomb lattice. (d) Random distribution. In panel (e), we plot the eigenenergies E_n for a square lattice with three different values of S . All three cases contain 1 zero-energy band. The number of positive-energy bands are 1, 3 and 8, for $S = \pi/2$, $3\pi/4$ and $8\pi/11$, respectively.

Therefore, $\phi^{(j)}(z_{m,n})$ represent the wave functions of zero-energy states. The density profile corresponding to $\phi^{(j)}$ resembles a ring with a radius of $\sqrt{\frac{j+1}{\pi/S-1}}$. As a result, the density of states per unit area is $1/S-1/\pi$ which is consistent with the degeneracy derived above using the (over)completeness property of the coherent states.

If we ignore the phase factor $(-1)^{m+n+mn}$, $\phi^{(j)}$ take the same form as the wave function of a charged particle in the lowest Landau level (LLL) confined in the (x, y) -plane subjected to a perpendicular magnetic field B :

$$\phi_{\text{LLL}}^{(j)}(x, y) = (x + iy)^j e^{-eB(x^2+y^2)/4\hbar}. \quad (5)$$

Note that previous studies have used the (over)completeness of coherent states to investigate the properties of LLL [12, 13]. Like ϕ_{LLL} , $\phi^{(j)}$ also possesses continuous translational symmetry, though defined on a lattice, because $e^{-\frac{\pi}{S-1}(z_{m,n}^*z - z_{m,n}z^*)}\phi^{(j)}(z_{m,n} - z)$ is also a zero-energy state for arbitrary $z \in \mathbb{C}$ [9]. Nevertheless, $\phi^{(j)}$ and ϕ_{LLL} can be distinguished by the Hall velocity v_H . For ϕ_{LLL} , v_H is inversely proportional to B . Whereas for $\phi^{(j)}$, supposing all $\phi^{(j)}$'s are filled by spinless fermions, the Hall conductivity is invariant with respect to S since the gap remains open for $S < \pi$, so v_H must be inversely proportional to the density of zero-energy states $1/S - 1/\pi$ rather than B . From another point of view, comparing the exponential factor of $\phi^{(j)}$ with that of ϕ_{LLL} , we can identify $\pi/S - 1$, up to a factor provided by the unit of length, as the effective magnetic field for the former. Thus in our lattice model, v_H is inversely proportional to the effective field rather than the true gauge field.

To numerically verify this argument, we perform the following calculation. We initially prepare a wavepacket, $\phi^{(0)}$, in the zero-energy ground band localized at the center of an 81×81 square lattice. We then add a linear potential, with gradient U , along the y -axis at $t = 0$, and the ensuing evolution of the wavepacket is depicted in Fig. 2. Fig. 2(a) show the snapshots of density profiles at various times. The three columns correspond to $S = \pi/4$, $\pi/2$ and $3\pi/4$ from left to right. One can see that the wavepacket disperses and moves along the x -axis, perpendicular to the direction of the linear potential. The evolution of the center position \bar{x} along the x -axis is plotted in the left panel of Fig. 2(b). \bar{x} is almost perfectly linear in time, which results from the very accurate quantization of the Hall conductivity. We can readily extract the Hall velocities, $v_H = 5 \times 10^{-4}$, 7.5×10^{-4} , 1.5×10^{-3} respectively. The Hall conductivity, given by $v_H(1 - S/\pi)/U$, is equal to 1 with a relative standard deviation on the order 10^{-7} for all three cases. As the wavepacket moves, it also disperses along the x -axis (but not along the y -axis). The right panel of Fig. 2(b) displays the evolution of the half width σ along the x -axis. The slower the wavepacket moves, the faster it disperses. Note that the LLL wavepacket $\phi_{\text{LLL}}^{(0)}$ is non-dispersive under a similar situation. In Fig. 2(c), we also display the evolution of a localized wavepacket for $S = 5\pi/4$. In this case, the wavepacket disperses fast in both directions, in stark contrast against the situation depicted in Fig. 2 where $S < \pi$. More snapshots for longer time scales are provided in the Supplemental Material [9].

Having thoroughly understood the zero-energy band, we now turn to investigate the full band structure of G^S (More details can be found in the Supplemental Material [9]). Let us take $S = p\pi/q$ where p, q are co-prime positive integers. After a gauge transformation $|m, n\rangle \rightarrow e^{-imnS} |m, n\rangle$, $G^S \rightarrow G'^S$, the Hamiltonian

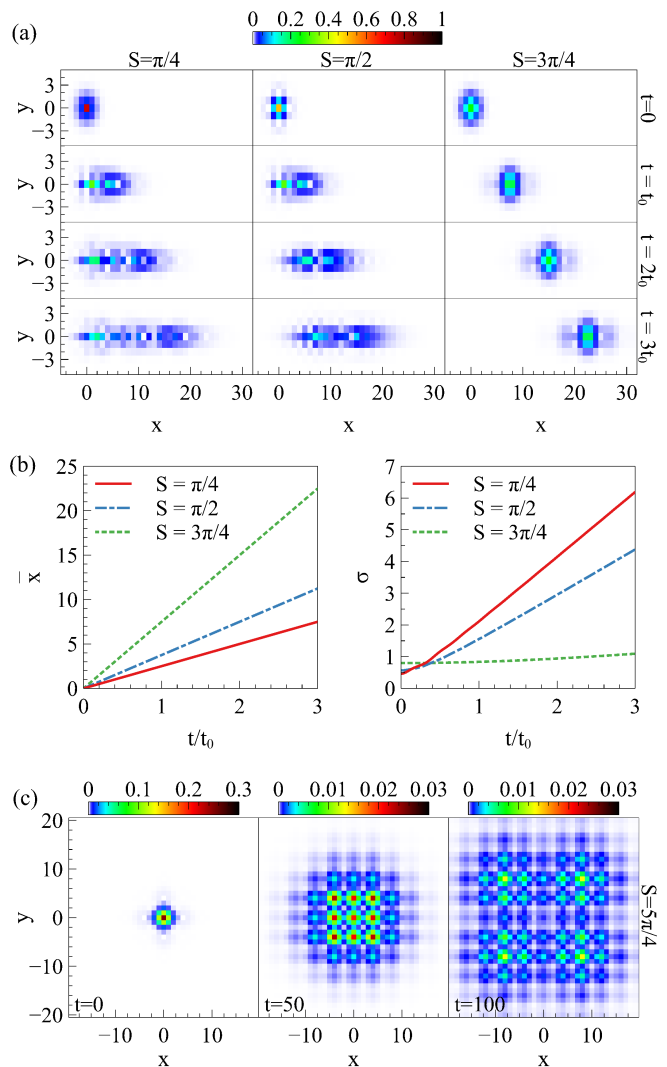


FIG. 2. (Color online) (a) Evolution of the density profile of a wavepacket on an $L \times L = 81 \times 81$ square lattices with a linear potential along the y -axis with gradient U . The evolution operator is given by $\exp\{-2\pi it(G^S + Uy)\}$, where we take $U = 3.75 \times 10^{-4}$. The positions x and y are renormalized by the lattice constant. The initial wavepacket is obtained by projecting a completely localized state to the lowest (zero-energy) band. $t_0 = 5000$. (b) The evolution of the central position \bar{x} and the half width σ along the x direction of the wavepacket in (a). (c) The same evolution as that in (a) except that now $S = 5\pi/4$ such that the lowest band is not a flat band.

manifests discrete translational symmetry:

$$G'_{m'+q, n'; m+q, n}{}^S = G'_{m', n'+1; m, n'+1}{}^S = G'_{m', n'; m, n}{}^S, \quad (6)$$

Therefore G^S can be reduced to a $q \times q$ matrix $g^S(k, l)$ acting on the q sites which form superlattice cell with length- q , and k, l are pseudo momenta defined in the range $-\frac{1}{q} < k \leq \frac{1}{q}$, $-1 < l \leq 1$. The explicit matrix elements of $g^S(k, l)$ are given by:

$$g_{m',m}^{S=p\pi/q} = \sum_{r,s} \exp \left[-\frac{1}{2} |z_{qr+m-m',s}|^2 + i\pi [k(qr+m-m') + (l+(m+m')pq)s - prs] \right], \quad m, m' = 1, 2, \dots, q \quad (7)$$

and its trace is given by

$$\text{Tr} \left(g^{p\pi/q} \right) = q \sum_{m,n} e^{-\frac{1}{2} |z_{qm,qn}|^2 + i\pi q(km+ln+pmn)}. \quad (8)$$

The eigenstate $|\phi_{k,l}^S\rangle$ of G^S takes the form

$$|\phi_{k,l}^S\rangle = \sum_{m,n} e^{i\pi(km+ln+mnS/\pi)} u_{k,l}(m) |m,n\rangle, \quad (9)$$

where $u_{k,l}(m)$ is an eigenstate of $g^S(k,l)$ and has q -period: $u_{k,l}(m+q) = u_{k,l}(m)$. If we take another gauge transformation $|m,n\rangle \rightarrow e^{imnS} |m,n\rangle$, $G^S \rightarrow G''^S$, the manifested symmetry becomes

$$G''_{m'+1,n';m+1,n} = G''_{m',n'+q;m,n'+q} = G''_{m',n';m,n}, \quad (10)$$

which implies that each eigenvalue of G^S must be at least q -fold degenerate, where the degeneracy arises from the freedom of choosing the starting site of the length- q superlattice cell.

To proceed further, one in general needs to resort to numerical calculations. However, analytic results can be obtained for the following cases:

(1) When $q = 1$ (i.e., $S = p\pi$), $|\phi_{k,l}^{p\pi}\rangle$ is readily obtained because $g^{p\pi}$ is just a number given by Eq. (8) with $q = 1$, and correspondingly $u_{k,l}(m) = 1$. Explicitly,

$$|\phi_{k,l}^{p\pi}\rangle = \sum_{m,n} e^{i\pi(km+ln+mpn)} |m,n\rangle. \quad (11)$$

The completeness of coherent states together with the singlet sum rule Eq. (2) tells us that $g^{p\pi} = 0$ if and only if $p = 1$ and $k = l = 1$, and $|\phi_{1,1}^{p\pi}\rangle$ is the corresponding non-degenerate zero-energy state.

(2) In the case of a rectangular lattice with arbitrary aspect ratio ξ , the matrix elements of $g^{p\pi/q}$ are given by Jacobi θ -functions [9]. For example, for the case of $q = 2$, the 2×2 matrix $g^{p\pi/2}$ takes the form:

$$g^{p\pi/2}(k,l) = \sum_{i=0}^3 c_i \sigma^{(i)}, \quad (12)$$

$$c_0 = \theta_3(k; ip\xi) \theta_3(l; ip\xi^{-1}),$$

$$c_1 = \theta_2(k; ip\xi) \theta_4(l; ip\xi^{-1}),$$

$$c_2 = (-1)^{\frac{p+1}{2}} \theta_1(k; ip\xi) \theta_1(l; ip\xi^{-1}),$$

$$c_3 = -\theta_4(k; ip\xi) \theta_2(l; ip\xi^{-1}),$$

where $\sigma^{(i)}$'s are Pauli matrices ($\sigma^{(0)}$ is the identity matrix). The two eigenvalues are thus

$$\chi_{\pm}^{p\pi/2}(k,l) = c_0 \pm \sqrt{|c_1|^2 + |c_2|^2 + |c_3|^2}.$$

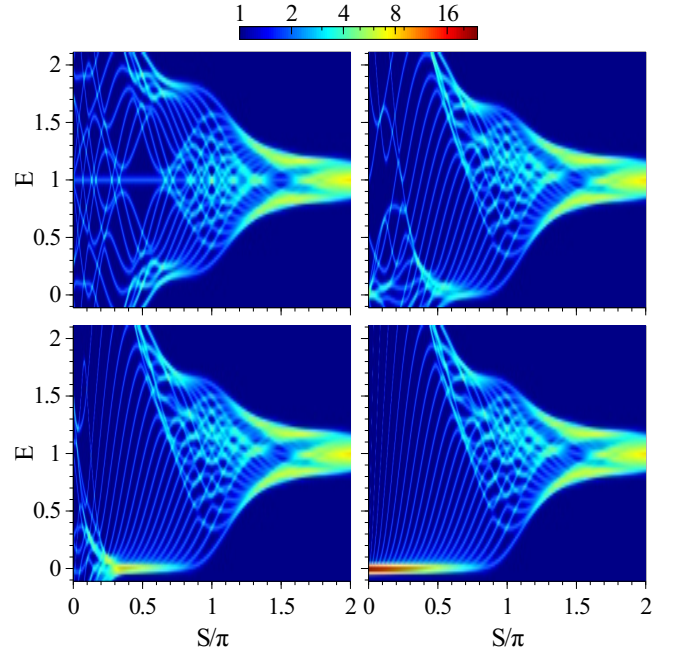


FIG. 3. (Color online) Spectrum for a 5×5 square lattice. The color map represents $(D+1)$ as in Fig. 1. (a) Only nearest-neighbor hoppings terms are kept. Here the G^S is identical to the Hofstadter model after a rescaling. (b) Nearest-neighbor and next-nearest-neighbor hoppings are kept. (c) Four hopping terms are kept. (d) All hopping terms are kept.

Especially when $p = 1$, one can show [9] that the lower eigenvalue $\chi_{-}^{p\pi/2} = 0$ independent of k and l . This leads to the massively degenerate zero-energy ground band, which contains half of all the eigenstates in this particular case. If we map the ground band to the Bloch sphere, we find that the wrapping number [14] (i.e., the Hall conductivity) is 1, which has been confirmed in Fig. (2).

In general, when $p < q$, $g^{p\pi/q}$ possesses zero eigenvalues. According to their degeneracy derived from the (over)completeness of coherent states, $g^{p\pi/q}$ must have $(q-p)$ zero eigenvalues. As a result, given $S = p\pi/q$, the spectrum contains p positive-energy bands and one zero-energy band, as shown in Fig. 1(e). However, we are not able to obtain an analytic proof of this property using just the matrix elements of g^S given in Eq. (7), except for the case with $p = 1$ and arbitrary q on rectangular lattices [9].

Finally, let us briefly discuss the experimental implementation of a Hamiltonian given by G^S . The key here is to engineer the desired hopping amplitude. Over the past few years, we have witnessed rapid progress in realizing lattice models in synthetic materials, particularly

synthetic dimensions, in both atomic [15–24] and photonic [25–35] systems, where the lattice sites are represented by different atomic states or photonic modes, respectively. Nearly arbitrary hopping amplitudes can be realized in such systems. Therefore, experimental realization of our model should in principle be within reach with current technologies. One important limitation of these synthetic systems is that the system size they can realize is always finite. To investigate the finite-size effect, we carried out the following study by considering a 5×5 square lattice. The spectrum is displayed in Fig. 3. In Fig. 3(a), we only include the nearest-neighbor hopping, and hence our model is identical to the Hofstadter model after a simple rescaling. The spectrum resembles the Hofstadter butterfly pattern. From Fig. 3(b) to (d) more higher-order hopping terms are included. One can see that the massively degenerate zero-energy flat band emerges as a result. This clearly demonstrates that the essential physics can be observed even in such a small system, which makes its experimental realization very promising.

Conclusion — We have proposed a new principle, based on the mathematical properties of Gram matrices, to construct model Hamiltonians supporting flat band. Previously, flat-band lattice models all require careful engineering of the lattice geometry. In our approach, remarkably, lattice geometry becomes irrelevant. In fact, numerical results represented by Fig. 1(d) shows that we do not even need a regular lattice. Using this principle, we constructed a particular model, in which the existence of the flat band depends on the completeness properties of the coherent states. The wave functions of the flat band states are universal, i.e., independent of the lattice geometry, and resemble the lowest Landau levels of a free particle in a gauge field. However, the two systems exhibit different Hall dynamics. We show that the essential features of our model can be observed in very small lattice systems with modest number of hopping terms, which facilitates their experimental implementation.

We acknowledge the support from the NSF and the Welch Foundation (Grant No. C-1669).

[1] R. B. Laughlin, *Phys. Rev. Lett.* **50**, 1395 (1983).
 [2] J. K. Jain, *Phys. Rev. Lett.* **63**, 199 (1989).
 [3] H. L. Stormer, D. C. Tsui, and A. C. Gossard, *Rev. Mod. Phys.* **71**, S298 (1999).
 [4] O. Derzhko, J. Richter, and M. Maksymenko, *Int. J. Mod. Phys. B* **29**, 1530007 (2015).
 [5] D. Leykam, A. Andreanov, and S. Flach, *Adv. Phys.: X* **3**, 1473052 (2018).
 [6] A. M. Perelomov, *Theor. Math. Phys.* **6**, 156 (1971).

[7] E. Kapit and E. Mueller, *Phys. Rev. Lett.* **105**, 215303 (2010).
 [8] We derive the Kapit-Mueller model in the Supplemental Material [9] and point out that there is an error in calculating the flux per unit cell in Ref. [7].
 [9] Supplemental Material, which contains more technical details such as the basics of Gram matrix, the discussion on the Kapit-Mueller model [7], the detailed derivation of the zero-energy wave functions and the band structure of our model, and Hall dynamics at longer time scale.
 [10] D. R. Hofstadter, *Phys. Rev. B* **14**, 2239 (1976).
 [11] R. Laughlin, *Ann. Phys.* **191**, 163 (1989).
 [12] D. J. Thouless, *J. of Phys. C: Solid State Phys.* **17**, L325 (1984).
 [13] R. Tao, *J. of Phys. C: Solid State Phys.* **19**, L619 (1986).
 [14] M. Z. Hasan and C. L. Kane, *Rev. Mod. Phys.* **82**, 3045 (2010).
 [15] A. Celi, P. Massignan, J. Ruseckas, N. Goldman, I. B. Spielman, G. Juzeliūnas, and M. Lewenstein, *Phys. Rev. Lett.* **112**, 043001 (2014).
 [16] M. Mancini, G. Pagano, G. Cappellini, L. Livi, M. Rider, J. Catani, C. Sias, P. Zoller, M. Inguscio, M. Dalmonte, and L. Fallani, *Science* **349**, 1510 (2015).
 [17] B. K. Stuhl, H.-I. Lu, L. M. Ayccock, D. Genkina, and I. B. Spielman, *Science* **349**, 1514 (2015).
 [18] T.-S. Zeng, C. Wang, and H. Zhai, *Phys. Rev. Lett.* **115**, 095302 (2015).
 [19] S. Barbarino, L. Taddia, D. Rossini, L. Mazza, and R. Fazio, *New J. Phys.* **18**, 035010 (2016).
 [20] B. Sundar, M. Thibodeau, Z. Wang, B. Gadway, and K. R. A. Hazzard, *Phys. Rev. A* **99**, 013624 (2019).
 [21] B. Sundar, B. Gadway, and K. R. Hazzard, *Sci. Rep.* **8**, 1 (2018).
 [22] F. A. An, E. J. Meier, J. Ang'ong'a, and B. Gadway, *Phys. Rev. Lett.* **120**, 040407 (2018).
 [23] M. Lohse, C. Schweizer, H. M. Price, O. Zilberberg, and I. Bloch, *Nature* **553**, 55 (2018).
 [24] S. Sugawa, F. Salces-Carcoba, A. R. Perry, Y. Yue, and I. Spielman, *Nature* **360**, 1429 (2018).
 [25] E. Lustig, S. Weimann, Y. Plotnik, Y. Lumer, M. A. Bandres, A. Szameit, and M. Segev, *Nature* **567**, 356 (2019).
 [26] D. Jukić and H. Buljan, *Phys. Rev. A* **87**, 013814 (2013).
 [27] X.-W. Luo, X. Zhou, C.-F. Li, J.-S. Xu, G.-C. Guo, and Z.-W. Zhou, *Nat. Commun.* **6**, 1 (2015).
 [28] L. Yuan, Y. Shi, and S. Fan, *Opt. Lett.* **41**, 741 (2016).
 [29] T. Ozawa, H. M. Price, N. Goldman, O. Zilberberg, and I. Carusotto, *Phys. Rev. A* **93**, 043827 (2016).
 [30] L. Yuan, Q. Lin, M. Xiao, and S. Fan, *Optica* **5**, 1396 (2018).
 [31] X.-F. Zhou, X.-W. Luo, S. Wang, G.-C. Guo, X. Zhou, H. Pu, and Z.-W. Zhou, *Phys. Rev. Lett.* **118**, 083603 (2017).
 [32] R. Ma, C. Owens, A. LaChapelle, D. I. Schuster, and J. Simon, *Phys. Rev. A* **95**, 062120 (2017).
 [33] S. Wang, X.-F. Zhou, G.-C. Guo, H. Pu, and Z.-W. Zhou, *Phys. Rev. A* **100**, 043817 (2019).
 [34] B. M. Anderson, R. Ma, C. Owens, D. I. Schuster, and J. Simon, *Phys. Rev. X* **6**, 041043 (2016).
 [35] N. Schine, A. Ryou, A. Gromov, A. Sommer, and J. Simon, *Nature* **534**, 671 (2016).

Supplemental Material: Gram Matrices, Coherent States, and Hofstadter Butterfly with Flat Band

Youjiang Xu and Han Pu

Department of Physics and Astronomy, and Rice Center for Quantum Materials,
Rice University, Houston, Texas 77251-1892, USA

In this Supplemental Material, we provide further technical details.

I. THE BASICS OF GRAM MATRIX

Given a set of vectors $|\nu_n\rangle$'s, $n = 1, 2, 3, \dots$ and their inner product $\langle \cdot | \cdot \rangle$, the corresponding Gram matrix (GM) G is given by

$$G_{m,n} := \langle v_m | v_n \rangle$$

G is hermitian and positive semi-definite, because any quadratic form $\sum_{m,n} x_m^* G_{m,n} x_n$ gives the norm of the vector $\sum_n x_n |v_n\rangle$.

We are interested in the case where $|\nu_n\rangle$'s are normalized, that is, $G_{n,n} \equiv 1$. G can be diagonalized by a unitary matrix U , $G_{m,n} = \sum_l U_{m,l} \lambda_l U_{n,l}^*$. The eigenvalues λ_l can be geometrically interpreted as a weight of projection. To see that, define orthonormal basis

$$|u_n\rangle := \sum_m U_{m,n} |v_m\rangle / \sqrt{\lambda_n}$$

If we project $|v_n\rangle$ onto the space spanned by $\{|u_m\rangle | m \in M\}$, then the norm $\rho_n^{(M)}$ of the projected $|v_n\rangle$

satisfies

$$\begin{aligned} \sum_n \rho_n^{(M)} &= \sum_n \sum_{m \in M} |\langle v_n | u_m \rangle|^2 \\ &= \sum_n \sum_{m \in M} \left| \sum_k U_{k,m} G_{n,k} / \sqrt{\lambda_m} \right|^2 \\ &= \sum_n \sum_{m \in M} |U_{n,m}|^2 \lambda_m \\ &= \sum_{m \in M} \lambda_m \end{aligned}$$

Consequently, the dimension of G equals the number of zero eigenvalues of G plus the dimension of the space spanned by $|\nu_n\rangle$'s.

II. DERIVE THE KAPIT-MUELLER MODEL

For a square lattice, the GM G^S in Eq. (1) of the main text is given by

$$G_{m'n',mn}^S = \exp(- (x^2 + y^2 - 2i(m'y - n'x)) S/2)$$

where $x := m - m'$, $y := n - n'$. The gauge transformation $|m, n\rangle \rightarrow (-1)^{m+n+mn} |m, n\rangle$ transforms G^S into

$$\begin{aligned} G_{m'n',mn}^S &= (-1)^{x+y+mn+m'n'} \exp(- (x^2 + y^2 - 2i(m'y - n'x)) S/2) \\ &= (-1)^{x+y+mn+m'n'-m'n-n'm} \exp(- (x^2 + y^2 - 2i(m'y - n'x)) S/2 + i\pi(m'n - n'm)) \\ &= (-1)^{x+y+xy} \exp\left(-\frac{\pi S}{2} (x^2 + y^2) + i\pi \left(1 - \frac{S}{\pi}\right) (m'y - n'x)\right) \end{aligned}$$

Now $t^{-1}(G^S - 1)$ is identical with J in Eq. (1) of Ref. [1]. The authors of Ref. [1], however, did not count the factor $(-1)^{x+y+xy}$ into the gauge field, so they incorrectly claimed that the flux per unit cell to be $2(\pi - S)$. The the factor properly taken into account, the correct flux per unit cell should be $2S$.

III. THE ZERO-ENERGY WAVE FUNCTIONS

Here we derive the explicit form of the wave functions of the zero-energy states when $S < \pi$, which is given in Eq. (4) in the main text. Suppose $z_{m,n}$'s build a lattice whose unit cell area is S ($S < \pi$), and $\alpha_{m,n} := \sqrt{\pi/S} z_{m,n}$ therefore build a lattice with unit cell area π . To prove that the following wave function

$$\psi_z^{(j)}(m, n) := (-1)^{m+n+mn} (z_{m,n} - z)^j \exp\left(-\frac{\pi/S - 1}{2} |z_{m,n} - z|^2 - \frac{\pi/S - 1}{2} (z_{m,n}^* z - z_{m,n} z^*)\right)$$

is an eigenstate of G^S with eigenvalue zero, we apply G^S on $\psi_z^{(j)}$ and get

$$\begin{aligned}
& \sum_{m,n} G_{m',n';m,n}^S \psi_z^{(j)}(m,n) \\
&= \sum_{m,n} \exp\left(-|z_{m,n} - z_{m',n'}|^2/2 + i \operatorname{Im} z_{m',n'}^* z_{m,n}\right) \\
&\quad \times (-1)^{m+n+mn} (z_{m,n} - z)^j \exp\left(-\frac{\pi/S-1}{2}|z_{m,n} - z|^2 - \frac{\pi/S-1}{2}(z_{m,n}^* z - z_{m,n} z^*)\right) \\
&\propto \sum_{m,n} (z_{m,n} - z)^j \exp\left(-\frac{\pi/S}{2}|z_{m,n}|^2 - \frac{1}{2}|z_{m',n'}|^2 + (z_{m',n'}^* + (\pi/S-1)z^*)z_{m,n}\right) \\
&\propto \sum_{m,n} \left(\alpha_{m,n} - \sqrt{\pi/S}z\right)^j \exp\left(-\frac{1}{2}|\alpha_{m,n}|^2 + \sqrt{\frac{S}{\pi}}(z_{m',n'}^* + (\pi/S-1)z^*)\alpha_{m,n}\right) \\
&= \sum_{k=0}^j \frac{j!}{k!(j-k)!} \left(-\sqrt{\pi/S}z\right)^{j-k} f^{(k)}\left(\sqrt{\frac{S}{\pi}}(z_{m',n'}^* + (\pi/S-1)z^*)\right)
\end{aligned}$$

where $f^{(k)}(z) := \frac{d^k}{dz^k} f(z)$ and

$$f(z) := \sum_{m,n} (-1)^{m+n+mn} \exp\left(-\frac{|\alpha_{m,n}|^2}{2} + \alpha_{m,n}z\right)$$

However, Perelomov has proved that [2] $f(z) = 0$ for arbitrary z . As a result, we have

$$\sum_{m,n} G_{m',n';m,n}^S \psi_z^{(j)}(m,n) = 0$$

In other words, $\psi_z^{(j)}(m,n)$ is an eigenfunction of G^S with eigenvalue 0. When $z = 0$, $\psi_z^{(j)}(m,n)$ reduces to Eq. (4) in the main text.

IV. THE BAND STRUCTURE OF G^S

Consider the case $S = p\pi/q$ where p, q are coprime positive integers. The translational symmetry of G^S is manifested when we apply gauge transformation $|m,n\rangle \rightarrow \exp(\mp imnS)|m,n\rangle$

$$\begin{aligned}
G_{m',n';m,n}^S &= \exp\left(-\frac{1}{2}|z_{m-m',n-n'}|^2 + i \operatorname{Im} z_{m',n'}^* z_{m,n}\right) \\
&= \exp\left(-\frac{1}{2}|z_{m-m',n-n'}|^2 - iS(mn' - m'n)\right) \\
&\rightarrow \exp\left(-\frac{1}{2}|z_{m-m',n-n'}|^2 - iS(mn' - m'n \mp mn \pm m'n')\right) \\
&= \exp\left(-\frac{1}{2}|z_{m-m',n-n'}|^2 \pm i\pi(m \pm m')(n \mp n')p/q\right)
\end{aligned}$$

If we choose the upper sign, the transformed G^S is invariant under the translations, $|m\rangle \rightarrow |m+q\rangle$ or $|n\rangle \rightarrow |n+1\rangle$ so the eigenstates of G^S must be in the form of

$$\begin{aligned}
|\phi_{k,l}^S\rangle &= \sum_{m,n} \exp(i\pi(km + ln + mnp/q)) u_{k,l}^S(m) |m,n\rangle \\
u_{k,l}^S(m+q) &= u_{k,l}^S(m)
\end{aligned}$$

where $-q^{-1} < k \leq q^{-1}$ and $-1 < l \leq 1$. Due to the symmetry of G^S in the other gauge, $|\phi_{k,l}^S\rangle$ must remain an eigenstate of the same eigenvalue if it is transformed as follows:

$$\begin{aligned} |\phi_{k,l}^S\rangle &\rightarrow \sum_{m,n} \exp(i\pi(k(m+c) + ln + 2(m+c)np/q - mnp/q)) u_{k,l}^S(m+c) |m,n\rangle \\ &= \exp(i\pi ck) \sum_{m,n} \exp\left(i\pi\left(km + \left(l + \frac{2cp}{q}\right)n + mnp/q\right)\right) u_{k,l}^S(m+c) |m,n\rangle \end{aligned}$$

Thus we obtain q orthogonal states by taking $c = 1, 2, \dots, q$, which means each eigenstate of G^S is at least q -fold degenerate.

The symmetries reduce G^S to a $q \times q$ matrix g^S whose eigenstates are $u_{k,l}^S$.

$$\begin{aligned} g_{m',m}^S &= \sum_{r,s} \exp\left(-\frac{1}{2}|z_{qr+m-m',s}|^2 + i\pi(k(qr+m-m') + (l+(m+m')p/q)s - prs)\right) \\ &1 \leq m, m' \leq q \end{aligned}$$

The trace of g^S has a compact form

$$\begin{aligned} \text{Tr}(g^S) &= \sum_{r,s} \exp\left(-\frac{1}{2}|z_{qr,s}|^2 + i\pi(kqr + ls - prs)\right) \sum_{m=1}^q \exp(2i\pi msp/q) \\ &= q \sum_{r,s} \exp\left(-\frac{1}{2}|z_{qr,qs}|^2 + i\pi q(kr + ls + prs)\right) \end{aligned}$$

When $p < q$, according to the degeneracy of the ground states, g^S must have $q - p$ zero eigenvalues. Therefore, $\text{Tr}(g^S)/p$ is the average energy of the excited states of given (k, l) for $p < q$.

When $q = 1$, we readily obtain

$$|\phi_{k,l}^{p\pi}\rangle = \sum_{m,n} \exp(i\pi(km + ln + mnp)) |m,n\rangle$$

and the only entry of g^S gives the eigenvalue

$$g^{p\pi} = \sum_{r,s} \exp\left(-\frac{1}{2}|z_{r,s}|^2 + i\pi(kr + ls + prs)\right)$$

If $S = \pi$, g^π vanishes at $(k, l) = (1, 1)$.

From now on, consider only the rectangular lattices. If the cells have aspect ratio ξ , we can use Jacobi θ -functions

$$\begin{aligned} \theta_1(z, \tau) &:= \sum_n \exp\left(\pi i \tau (n + 1/2)^2 + 2i\pi \left(z - \frac{1}{2}\right) (n + 1/2)\right) \\ \theta_2(z, \tau) &:= \sum_n \exp\left(\pi i \tau (n + 1/2)^2 + 2i\pi z (n + 1/2)\right) \\ \theta_3(z, \tau) &:= \sum_n \exp\left(\pi i \tau n^2 + 2i\pi z n\right) \\ \theta_4(z, \tau) &:= \sum_n \exp\left(\pi i \tau n^2 + 2i\pi \left(z - \frac{1}{2}\right) n\right) \end{aligned}$$

to represent g^S as follows

$$\begin{aligned}
g_{m',m}^S &= \sum_{r,s} \exp \left(-\frac{S}{2} \left(\xi (qr + m - m')^2 + \xi^{-1} s^2 \right) + i\pi \left(k(qr + m - m') + (l + (m + m')p/q)s - prs \right) \right) \\
&= \exp \left(-\frac{S\xi(m-m')^2}{2} + i\pi k(m-m') \right) \\
&\quad \times \sum_{r,s} \exp \left(-\frac{S}{2} \left(\xi q^2 r^2 + \xi^{-1} s^2 \right) + 2i\pi \left(\frac{q(k + i\xi(m-m')p/q)}{2} r + (l + (m + m')p/q) \frac{s}{2} - \frac{prs}{2} \right) \right) \\
&= \exp \left(-\frac{S\xi(m-m')^2}{2} + i\pi k(m-m') \right) \\
&\quad \times \sum_{r,s} \exp \left(-\frac{S}{2} \left(\xi q^2 r^2 + 4\xi^{-1} s^2 \right) + 2i\pi \left(\frac{q(k + i\xi(m-m')p/q)}{2} r + (l + (m + m')p/q) s \right) \right) \\
&\quad + \exp \left(-\frac{S}{2} \left(\xi q^2 r^2 + 4\xi^{-1} \left(s + \frac{1}{2} \right)^2 \right) + 2i\pi \left(\frac{q(k + i\xi(m-m')p/q) - p}{2} r + (l + (m + m')p/q) \left(s + \frac{1}{2} \right) \right) \right) \\
&= \exp \left(-\frac{S\xi(m-m')^2}{2} + i\pi k(m-m') \right) \sum_{\chi=0,1} \theta_{3+\chi(p \bmod 2)}(z_1, \tau_1) \theta_{3-\chi}(z_2, \tau_2)
\end{aligned}$$

where

$$\tau_1 := \frac{ipq\xi}{2}, \quad \tau_2 := \frac{2ip}{q\xi}, \quad z_1 := \frac{qk}{2} + \frac{(m-m')\tau_1}{q}, \quad z_2 := l + \frac{(m+m')p}{q}$$

Especially, when $q = 2$ (hence p must be odd), we have

$$\begin{aligned}
g_{m',m}^{p\pi/2} &= \exp \left(-\frac{p\pi\xi(m-m')^2}{4} + i\pi k(m-m') \right) \\
&\quad \times \left(\begin{aligned} &\theta_3 \left(k + \frac{(m-m')ip\xi}{2}, ip\xi \right) \theta_3 \left(l + \frac{(m+m')p}{2}, ip\xi^{-1} \right) \\ &+ \theta_4 \left(k + \frac{(m-m')ip\xi}{2}, ip\xi \right) \theta_2 \left(l + \frac{(m+m')p}{2}, ip\xi^{-1} \right) \end{aligned} \right)
\end{aligned}$$

or equivalently

$$\begin{aligned}
g^{p\pi/2} &= \theta_3(k, ip\xi) \theta_3(l, ip\xi^{-1}) - \sigma^{(3)} \theta_4(k, ip\xi) \theta_2(l, ip\xi^{-1}) \\
&\quad + \sigma^{(1)} \theta_2(k, ip\xi) \theta_4(l, ip\xi^{-1}) + \sigma^{(2)} (-1)^{\frac{p+1}{2}} \theta_1(k, ip\xi) \theta_1(l, ip\xi^{-1})
\end{aligned}$$

where σ 's are Pauli matrices. Apparently, the eigenvalues $\lambda_{\pm}^{p\pi/2}$ of $g^{p\pi/2}$ are

$$\begin{aligned}
\lambda_{\pm}^{p\pi/2} &= \theta_3(k, ip\xi) \theta_3(l, ip\xi^{-1}) \\
&\quad \pm \sqrt{\theta_2^2(k, ip\xi) \theta_4^2(l, ip\xi^{-1}) + \theta_4^2(k, ip\xi) \theta_2^2(l, ip\xi^{-1}) + \theta_1^2(k, ip\xi) \theta_1^2(l, ip\xi^{-1})}
\end{aligned}$$

The completeness of coherent states guarantees $\lambda_{-}^{\pi/2} = 0$, so $\lambda_{+}^{\pi/2} = 2\theta_3(k, i\xi) \theta_3(l, i\xi^{-1})$.

In order to verify $\lambda_{-}^{\pi/2} = 0$, we will show that $g^{\pi/q}$ is rank-1 without referring to the completeness of coherent states. Now $p = 1$, $\tau_1 = -\tau_2^{-1}$, so we can use Jacobi identities

$$\theta_{3+\chi} \left(\frac{z}{\tau}, -\frac{1}{\tau} \right) = (-i\tau)^{1/2} \exp(i\pi z^2/\tau) \theta_{3-\chi}(z, \tau), \quad \chi = 0, \pm 1$$

to recast $g^{\pi/q}$ as follows

$$g_{m',m}^{\pi/q} = (-i\tau_2)^{1/2} \exp \left(-\frac{S\xi(m-m')^2}{2} + i\pi k(m-m') + i\pi z_1^2 \tau_2 \right) \sum_{\chi=0,1} \theta_{3-\chi}(z_1 \tau_2) \theta_{3-\chi}(z_2)$$

where we have omitted the second argument τ_2 of the θ -functions. Define

$$R_{m,m'} := (-i\tau_2)^{-1} \exp\left(S\xi(m-m')^2 - 2i\pi(k(m-m') + z_1^2\tau_2)\right) \left(g_{m',m}^{\pi/q} g_{m'+1,m+1}^{\pi/q} - g_{m'+1,m}^{\pi/q} g_{m',m+1}^{\pi/q}\right)$$

$R \equiv 0$ iff $g^{\pi/q}$ is rank-1. Representing $g^{\pi/q}$ by θ -functions, we get

$$\begin{aligned} R_{m,m'} &= \sum_{\chi,\chi'} \theta_{3-\chi}(z_1\tau_2) \theta_{3-\chi}(z_2) \theta_{3-\chi'}(z_1\tau_2) \theta_{3-\chi'}\left(z_2 + \frac{2}{q}\right) \\ &\quad - \theta_{3-\chi}\left(z_1\tau_2 + \frac{1}{q}\right) \theta_{3-\chi}\left(z_2 + \frac{1}{q}\right) \theta_{3-\chi'}\left(z_1\tau_2 - \frac{1}{q}\right) \theta_{3-\chi'}\left(z_2 + \frac{1}{q}\right) \end{aligned}$$

To proceed, we need the sum rules of θ -functions.

$$\begin{aligned} &\theta_2(v+w) \theta_2(v-w) \theta_2(x+y) \theta_2(x-y) - \theta_2(x+w) \theta_2(x-w) \theta_2(v+y) \theta_2(v-y) \\ &= \theta_1(v+x) \theta_1(v-x) \theta_1(y+w) \theta_1(y-w) \end{aligned}$$

$$\begin{aligned} &\theta_3(v+w) \theta_3(v-w) \theta_3(x+y) \theta_3(x-y) - \theta_3(x+w) \theta_3(x-w) \theta_3(v+y) \theta_3(v-y) \\ &= -\theta_1(v+x) \theta_1(v-x) \theta_1(y+w) \theta_1(y-w) \end{aligned}$$

$$\begin{aligned} &\theta_2(v+w) \theta_3(v-w) \theta_3(x+y) \theta_2(x-y) - \theta_2(x+w) \theta_3(x-w) \theta_3(v+y) \theta_2(v-y) \\ &= -\theta_4(v+x) \theta_1(v-x) \theta_1(y+w) \theta_4(y-w) \end{aligned}$$

If we take

$$v = z_1\tau_2, \quad w = 0, \quad x = z_2 + \frac{1}{q}, \quad y = \frac{1}{q}$$

then

$$\begin{aligned} R_{m,m'} &= \sum_{\chi,\chi'=0,1} \theta_{3-\chi}(v+w) \theta_{3-\chi'}(v-w) \theta_{3-\chi'}(x+y) \theta_{3-\chi}(x-y) \\ &\quad - \theta_{3-\chi'}(x+w) \theta_{3-\chi}(x-w) \theta_{3-\chi}(v+y) \theta_{3-\chi'}(v-y) \\ &= 0 \end{aligned}$$

So we have proved that, for rectangular lattice with aspect ratio ξ , $g^{\pi/q}$ has only one positive eigenvalue:

$$\begin{aligned} \text{Tr}\left(g^{\pi/q}\right) &= q \sum_{r,s} \exp\left(-\frac{1}{2}|z_{qr,qs}|^2 + i\pi q(kr + ls - rs)\right) \\ &= q \sum_{\chi=0,1} \theta_{3+\chi(q \bmod 2)}\left(\frac{qk}{2}, \frac{iq\xi}{2}\right) \theta_{3-\chi}\left(ql, \frac{2iq}{\xi}\right) \end{aligned}$$

V. SNAPSHOTS OF THE HALL DYNAMICS FOR $S = 3\pi/4$ SQUARE LATTICE

Figure 2 of the main text depicts the Hall dynamics: the evolution of a localized wavepacket initially at the center of the lattice under the effect of a linear potential along the y -axis. In our numerical calculation, we considered a finite-sized 81×81 square lattice. Hence eventually the wavepacket will encounter the boundary, at which time it will travel along the edges due to the presence of the edge or skipping modes, and return back to its original location. At the same time, the wavepacket disperses along the x -axis. The dynamics over a long time scale for $S = 3\pi/4$ is displayed in Fig. 1 below.

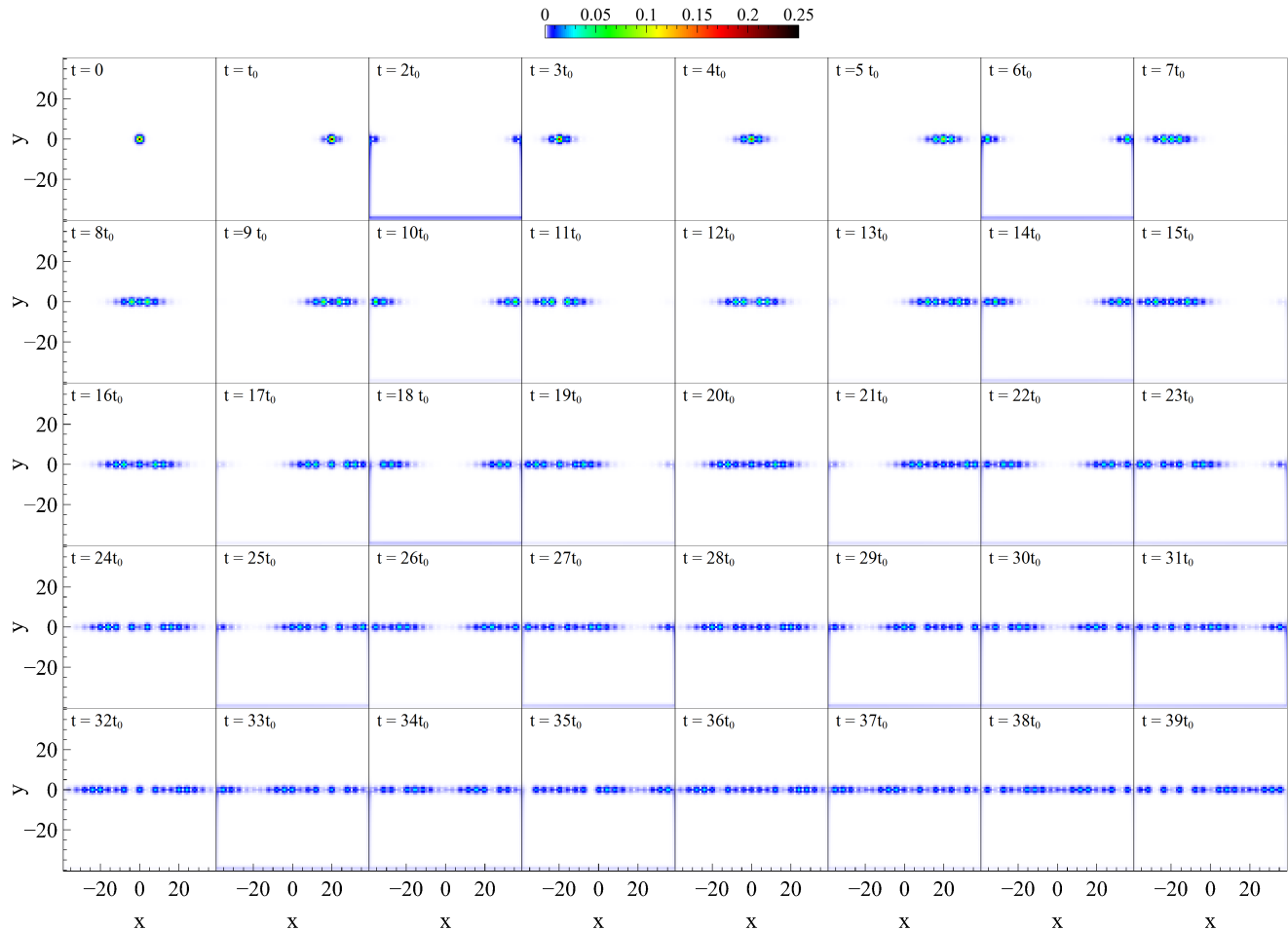


FIG. 1. (Color online) The same plot as Fig.2(a) in the main text except that $t_0 = 1.319 \times 10^4$ and $S = 3\pi/4$ for all panels. These snapshots show the dispersion of the wave packet during its propagation in the bulk and its tunneling through the edge modes. The quasi period is about $4t_0$.

-
- [1] E. Kapit and E. Mueller, *Phys. Rev. Lett.* **105**, 215303 (2010).
 [2] A. M. Perelomov, *Theor. Math. Phys.* **6**, 156 (1971).
-